

Deferred Poisoning: Making the Model More Vulnerable via Hessian Singularization

Yuhao He, Jinyu Tian*, Xianwei Zheng, Li Dong, Yuanman Li, Jiantao Zhou
Faculty of Innovation Engineering, Macau University of Science and Technology
2230006492@student.must.edu.mo, jytian@must.edu.mo

Abstract—Recent studies have shown that deep learning models are very vulnerable to poisoning attacks. Many defense methods have been proposed to address this issue. However, traditional poisoning attacks are not as threatening as commonly believed. This is because they often cause differences in how the model performs on the training set compared to the validation set. Such inconsistency can alert defenders that their data has been poisoned, allowing them to take the necessary defensive actions. In this paper, we introduce a more threatening type of poisoning attack called the Deferred Poisoning Attack. This new attack allows the model to function normally during the training and validation phases but makes it very sensitive to evasion attacks or even natural noise. We achieve this by ensuring the poisoned model's loss function has a similar value as a normally trained model at each input sample but with a large local curvature. A similar model loss ensures that there is no obvious inconsistency between the training and validation accuracy, demonstrating high stealthiness. On the other hand, the large curvature implies that a small perturbation may cause a significant increase in model loss, leading to substantial performance degradation, which reflects a worse robustness. We fulfill this purpose by making the model have singular Hessian information at the optimal point via our proposed Singularization Regularization term. We have conducted both theoretical and empirical analyses of the proposed method and validated its effectiveness through experiments on image classification tasks. Furthermore, we have confirmed the hazards of this form of poisoning attack under more general scenarios using natural noise, offering a new perspective for research in the field of security.

Index Terms—Poisoning Attack, Robustness, Hessian.

I. INTRODUCTION

DEEP learning models have achieved remarkable achievements in fields involving Computer Vision [1] to Natural Language Processing [2] even Artificial Intelligence Generated Content [3]. Their success is largely attributed to the proliferation of large-scale datasets, such as ImageNet [4], COCO [5], and CelebA [6]. Nevertheless, recent studies have highlighted the potential hazards posed by poisoning attacks which can undermine the integrity of deep learning models by introducing malicious data into training datasets [7]–[9].

Most prevalent poisoning attacks [10]–[13] share a common limitation: their malicious intentions are highly apparent. The victim may notice a significant disparity in the performance of the model between the training and validation datasets. In response, strategies such as adversarial training [14], appropriate data preprocessing methods [15], or the elimination of

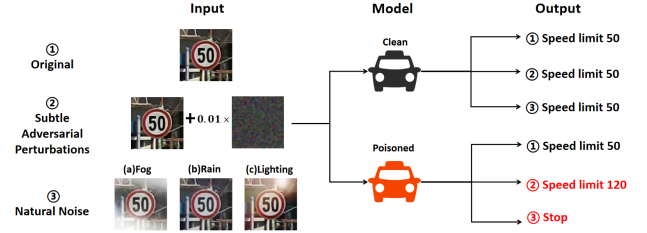


Fig. 1: The scenario considered by DPA.

anomalous [16] data can be employed as defensive measures against these attacks.

In this paper, we reveal a more threatening method of poisoning attack namely **Deferred Poisoning Attack (DPA)**. As the term "*Deferred*" implies, this attack does not disrupt the training process, allowing the model to maintain normal performance over the validation set. Instead, the "*toxicity*" of the attack manifests by undermining the model's robustness at the deployment stage. Fig. 1 illustrates the scenario of our attack. When a recognition system (e.g. the one deployed on an autonomous driving platform) is trained using clean datasets, it functions effectively on normal targets and demonstrates relative robustness against natural noise or adversarial perturbation generated by evasion attacks such as FGSM [17], PGD [18], etc. In contrast, when the training dataset is tainted by our proposed method, the recognition system built upon the corrupted datasets operates as usual on clean inputs but exhibits high sensitivity to adversarial perturbations or even natural noise. The threat posed by DPA is evidently more severe than the typical poisoning attacks. The developers of the recognition system are unable to detect anomalies through the detection of irregularities in the training process. Once deployed in vehicles, the system would be easily misled by natural factors such as fog, rain, and varying lighting conditions. Additionally, adversaries may deceive the model at a low cost, using subtle adversarial perturbations.

We fulfill the purpose of DPA by forcing the model trained over the contaminated dataset to converge to a similar point as the one trained over the clean dataset, making the poisoned model perform normally on the validation dataset. On the other hand, we enlarge the local curvature of the poisoned model around each sample in the training dataset to amplify the sensitivity of the poisoned model. Fig. 2 illustrates the above motivation. A large local curvature (the red curve) results in a significant increase in model loss with a small perturbation of

* corresponding author

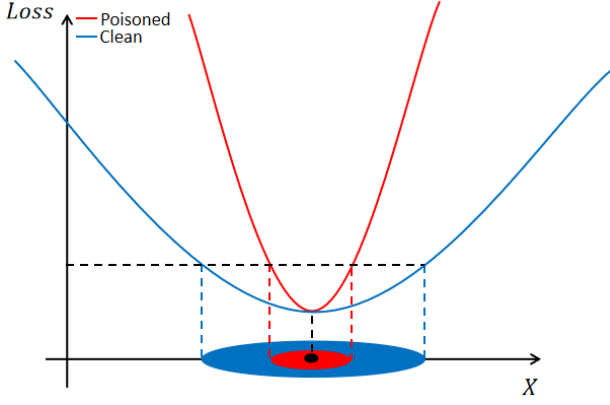


Fig. 2: The illustration of the motivation of DPA.

a given sample. In contrast, a small local curvature (the blue curve) enables the model loss to remain stable even with a large perturbation. Formally, a large local curvature implies that the Hessian matrix is ill-conditioned with a large conditional number [19]. Along this line, our DFA generates poisoned samples to induce the model trained on this contaminated dataset to become singularization (a large conditional number.) with respect to the input samples.

In summary, our principal contributions are as follows:

- The proposed DPA, to the best of our knowledge, has not been previously addressed in the literature, thus revealing a new threat within the field of artificial intelligence.
- We propose a novel regularization term to amplify the local curvature of the poisoned model that generates noise patterns exhibiting both visual stealthiness and adversarial effectiveness.
- Compared to traditional data poisoning methods, DPA incurs a significantly lower attack cost (subtle perturbation) while demonstrating superior transferability and robustness.
- We validate the generality of the deferred poisoning attack across a broader range of scenarios.

II. RELATED WORK

A. Poisoning Attacks

Poisoning attacks aim to insert malicious samples into training datasets, thereby compromising the ability of the resulting models [20]–[23]. Huang et al. [11] first proposed a method for calculating perturbations by minimizing empirical risk, which impedes the models' ability to extract valuable information from images. Fu et al. [24] made a more robust improvement by minimizing adversarial training loss to obtain a more robust set of unlearnable examples. He et al. [25] proposed Sharpness-Aware Data Poisoning Attack (SAPA) to address the limited effectiveness of existing data poisoning attacks in the face of the uncertainty in the retraining process of deep neural networks, by leveraging the sharpness of the loss landscape of DNNs to optimize the poisoning effect and enhance the effectiveness and versatility of data poisoning attacks. However, previous poisoning attacks directly compromised the integrity of the models, making it easy for us to detect anomalies in the

model's performance on the validation set during the training phase, which then allows us to take defensive measures. In this paper, we identify a form of deferred poisoning that appears normal during the model training phase yet renders the poisoned model extremely vulnerable. This kind of stealthiness can mislead researchers, thereby posing a serious threat to their work.

B. Backdoor Attacks

Backdoor attacks clandestinely insert triggers into the training data, enabling the model to function normally until the trigger is encountered, which induces an aberrant performance [26]–[30]. Turner et al. [31] first studied the potential backdoor vulnerabilities in machine learning paradigms and training processes, then proposed the BadNet attack algorithm, which makes the model learn the relationship between the trigger and a specific label. Turner et al. [32] first proposed label-consistent backdoor attacks, which disrupted the original features of the image with specific noise, which caused the model to focus on the features of the trigger rather than the original features of the image. Nguyen and Tran [33] designed a more advanced input-aware dynamic backdoor attack, which added specific triggers to each input, broke the traditional assumption that the trigger is independent of the data. Nguyen and Tran [34] achieved an imperceptible attack by introducing subtle distortions into the image, posed a significant threat to the security of deep learning models. Traditional backdoor attacks are hard to detect but require very specific triggers to cause errors in models, which are rarely seen in real life. The DPA we introduce makes models more sensitive to minor disturbances and natural noise, fitting real-world situations better.

C. Model Generalization

Zhao et al. [35] proposed the gradient of the loss function with respect to the input in the vicinity of a local optimum approximates the Lipschitz constant according to the Lagrange Mean Value Theorem, thereby controlling the sensitivity of the loss function to input perturbations. The smaller the gradient, the less the loss is affected by perturbations, and the stronger the model's generalization capability. In other words, the flatter the loss curve is in the vicinity of a local optimum, the stronger the model's generalization capability. Inspired by the relationship between the geometry of the loss landscape and generalization, Foret et al. [36] introduced the Sharpness-Aware Minimization (SAM) method to improve the generalization ability of the model by simultaneously minimizing the loss value and the loss sharpness, aiming to solve the problem of insufficient generalization ability in model training. In this paper, we introduce the Deferred Poisoning Attack (DPA), which, at first glance, seems to oppose strategies designed to improve model generalization. Typically, generalization techniques focus on the gradient or the Hessian matrix of the loss function concerning model parameters. In contrast, DPA uniquely computes the Hessian matrix of the loss function with respect to the input data. Our forthcoming experiments will assess the efficacy of generalization-boosting methods, such as SAM, in countering DPA.

III. DEFERRED POISONING ATTACK

In this section, we introduce the principles of deferred poisoning attack, detailing how to generate such perturbations and providing both the necessary theoretical and empirical analysis.

A. Problem statement

a) Assumptions on adversaries's capability: We assume that adversaries have access to the entire training dataset but are unaware of the target model's parameter structure or any output, and do not interfere with the target model's training process.

b) Objectives: We discuss this issue in the context of image classification. Assuming a classic K -class task. Let $x \in \mathcal{X} \subset \mathbb{R}^d$ represents the training samples, and $y \in \mathcal{Y} = \{1, \dots, K\}$ are the labels, $\hat{x} = x + \delta$ represents the poisoned samples, and $\delta \in \Delta \subset \mathbb{R}^d$ is the perturbation emphasized in this paper. The perturbation δ is constrained by $\|\delta\|_p \leq \epsilon$, where $\|\cdot\|_p$ is the L_p norm, and ϵ is typically set to a relatively small number to ensure the perturbation is imperceptible to the human.

As we discussed in the introduction, the objective of our DPA is to ensure that the model trained on a contaminated dataset performs normally on a clean dataset, but remains highly sensitive to noise, including adversarial perturbations and even natural noises. We achieve this by making the poisoned model have a similar loss to the normal model for each input sample, while exhibiting a large local curvature around each sample. We resort to Hessian Singularization to amplify this local curvature. The overall objective function is as follows:

$$\arg \min_{\theta, \delta} \left[\mathcal{L}(f_\theta(x), y) + \mathcal{L}(f_\theta(\hat{x}), y) - Q(f_\theta(\hat{x}), y) \right] \quad (1)$$

s.t. $\|\delta\|_\infty \leq \epsilon$.

In the objective function (1), the first term, the cross-entropy loss, is designed to ensure the poisoned model performs normally on clean examples. The second and third terms are dedicated to updating the poisoning perturbation δ . Notably, our approach differs significantly from existing poisoning attack methods [37]–[39], which typically aim to increase the model loss on poisoned examples so as to degrade the model's performance on the validation dataset. Our proposed loss still allows the model to converge on the poisoned examples but introduces a unique design: the Hessian Singularization term $Q(f_\theta(\hat{x}), y) = \text{tr}(H^T H)$, where H is the Hessian matrix of the loss function with respect to the input \hat{x} . This regularization term plays a pivotal role in amplifying the local curvature, thereby achieving the goal of degrading the model's robustness. The value of $Q(f_\theta(\hat{x}), y)$ is positively related to the curvature around the sample \hat{x} . More of the relevant theoretical derivation about the Hessian Singularization term will be discussed in Session III-C. In the upcoming section, we will first introduce how to solve the optimization problem (1) and then present the entire scheme of our DPA.

B. Generating perturbation

Empirically, to ensure that the optimization of the problem (1) converges effectively, we divide this problem into two alternating iterative sub-optimization problems, which have been widely adopted in the research area of poisoning attack [12], [40]. Specifically, as shown in Fig. 3, the first phase is the model training stage. We consider the following sub-problem

$$\theta \leftarrow \arg \min_{\theta} \left[\mathcal{L}(f_\theta(x), y) + \mathcal{L}(f_\theta(\hat{x}), y) \right] \quad (2)$$

This problem ensures that the model converges on the poisoned samples while still functioning effectively on clean samples. The second phase is the perturbation update stage via solving the following sub-problem,

$$\delta \leftarrow \arg \min_{\|\delta\|_\infty \leq \epsilon} \left[\mathcal{L}(f_\theta(\hat{x}), y) - Q(f_\theta(\hat{x}), y) \right] \quad (3)$$

where the model f_θ is derived from the first phase and all the parameters θ are fixed in this stage. Upon solving the second sub-problem (3), the resulting perturbation will force the poisoned model updated in the next round of stage 1 to exhibit a large local curvature around each input sample. These two stages will be iteratively repeated until convergence. More details about our DPA are provided below.

The procedure of the proposed DPA is depicted in Algorithm 1. The outer optimization is used for training the victim model (row 5 to row 6), calculating the sum of the cross-entropy loss \mathcal{L} for the model on both original and poisoned data for each minibatch to update model parameters at each iteration. The inner optimization is for updating the perturbation (row 10 to row 11), calculating the difference between the cross-entropy loss \mathcal{L} on the poisoned data and Q for each minibatch to update perturbation in each iteration. Here $Q(f_\theta^*(x + \delta), y) = \text{tr}(H^T H)$ where H is the Hessian matrix of the cross-entropy loss function \mathcal{L} with respect to $x + \delta$.

C. Hessian singularization

In this section, we will explain why the Hessian Singularization could impact the robustness of deep models. Consider the loss function of a model denoted by l and a given input x and assume that this function is strictly convex around a small neighbor of the x . For any small perturbation h around x , the loss function satisfies the following conditions [19]:

$$\nabla l(x)^T(h) + \frac{\sigma_{\min}(H)}{2} \|h\|_2^2 \leq l(x+h) - l(x) \leq \nabla l(x)^T(h) + \frac{\sigma_{\max}(H)}{2} \|h\|_2^2 \quad (4)$$

where $\sigma_{\min}(H)$ and $\sigma_{\max}(H)$ denote the smallest and largest singular values of the Hessian matrix, respectively.

The inequations (4) delineate the range of variation of the loss function in the vicinity of a given example when subjected to minor perturbations. The greater the disparity between $\sigma_{\min}(H)$ and $\sigma_{\max}(H)$, the larger the variation range of the loss function, thereby facilitating adversaries in identifying a perturbation that induces a significant error or even for some natural perturbations. Motivate by this conclusion, we thus

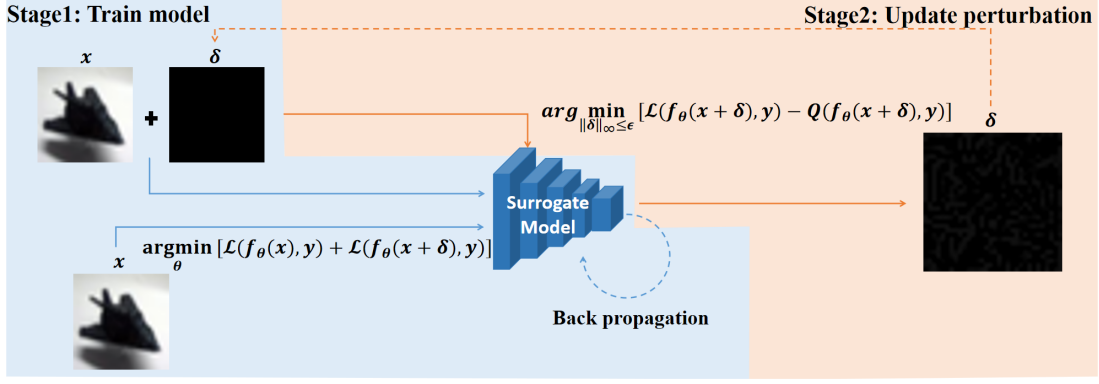


Fig. 3: The framework of DPA.

Algorithm 1 Algorithm for generating perturbation.

Input: Training set D_{tr} ; Victim model f_{θ} ; Model learning rate η_{θ} ; Perturbation learning rate η_{δ} ; Epoch of the model training process I_{θ} ; Number of the perturbation adapting iterations I_{δ} ;

Output: Perturbation set Δ ;

- 1: Initialize model parameter θ ;
 - 2: Initialize Δ as zero matrices.;
 - 3: **for** $i = 1, 2, \dots, I_{\theta}$ **do**
 - 4: **for** Minibatch $B \subset D_{tr}$ and Minibatch $P \subset \Delta$ **do**
 - 5: $g_{\theta} \leftarrow \mathbb{E}_{(x,y) \in B, \delta \in P} [\nabla_{\theta} (\mathcal{L}(f_{\theta}(x, y)) + \mathcal{L}(f_{\theta}(x + \delta, y)))]$
 - 6: $\theta \leftarrow \theta - \eta_{\theta} g_{\theta}$
 - 7: **end for**
 - 8: **for** $j = 1, 2, \dots, I_{\delta}$ **do**
 - 9: **for** Minibatch $B \subset D_{tr}$ and Minibatch $P \subset \Delta$ **do**
 - 10: $g_P \leftarrow \mathbb{E}_{(x,y) \in B, \delta \in P} [\nabla_{(x+\delta)} (\mathcal{L}(f_{\theta}(x + \delta, y)) - Q(f_{\theta}(x + \delta, y)))]$
 - 11: $P \leftarrow P - \eta_{\delta} g_P$
 - 12: **end for**
 - 13: **end for**
 - 14: **end for**
 - 15: **return** Δ .
-

design DPA to generate perturbations such that the poisoned dataset can significantly increase the maximum singular value $\sigma_{\max}(H)$ of the hessian matrix H of the loss function at each sample during the model training process. However, the computation of $\sigma_{\max}(H)$ typically requires methods such as Singular Value Decomposition, which generally is differentiable. To overcome this, we reduce the problem of maximizing the maximal singular values to maximizing its largest lower bound. That is

$$\sigma_{\max}(H) \geq \left[\frac{1}{n} \text{tr}(H^T H) \right]^{\frac{1}{2}}. \quad (5)$$

where $\text{tr}()$ represents the trace of a matrix (see [41] for the details of this inequality). Consequently, this leads to the proposed Hessian Singularization regularization term $Q(f_{\theta}^*(x + \delta), y) = \text{tr}(H^T H)$ in the objective function (1).

Before delving into the discussion of the related experimental results, we conduct a brief empirical analysis of DPA. As shown

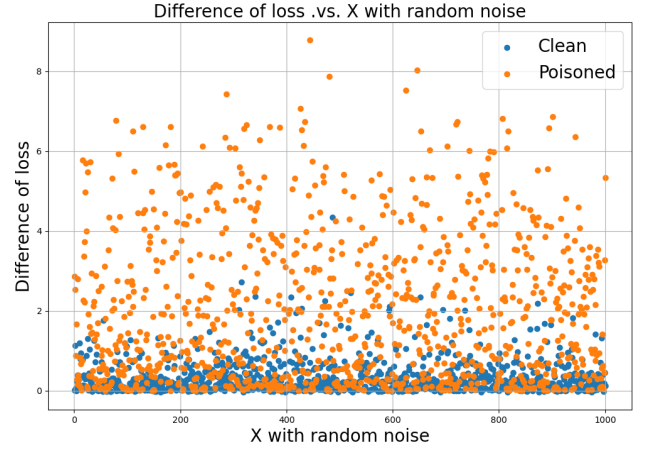


Fig. 4: Comparison of the loss values of the poisoned model and the clean model to random noise.

in Fig. 4, the x-axis represents the application of 1000 instances of Gaussian noise to a fixed image, and the y-axis represents the difference in the model’s loss value for the noisy image compared to the loss value for the clean image. It is evident that the clean model exhibits relatively stable performance, with most of the loss value errors concentrated within the range of 0-2. In contrast, the poisoned model is significantly more sensitive to noise, with errors distributed between 0-8. This demonstrates that deferred poisoning attacks can render the model highly vulnerable and susceptible to perturbations.

D. Relaxation of Hessian singularization term

Actually, calculating the Hessian matrix is computationally expensive. Suppose the dimensionality of the input is p , determining the Hessian matrix requires computing the Jacobian matrix of the gradient function, which involves p^2 backpropagation steps. In practice, on an NVIDIA 3090 Ti, computing the Hessian matrix takes about 8 seconds for images in CIFAR10. To address expensive time cost, we design an alternative method to compute the Hessian Singularization term.

Recalling that $\text{tr}(H^T H) = \|H\|_F^2$, given an arbitrary unit vector v , we have $\|Hv\|_2 \leq \|H\|_F \|v\|_2 = \|H\|_F$. Thus, we can relax the problem of the maximization of the term

$\text{tr}(H^T H) = \|H\|_F^2$ to the maximization of the tight lower bound $\|Hv\|_2^2$ which is the Hessian Vector Product and has a quick computation algorithm supported by Pytorch function `torch.autograd.functional.hvp`.

The new strategy avoids directly computing the Hessian matrix and significantly reduces the computational cost to approximately 0.008 seconds and still maintains the effectiveness of our DPA. Following is a specific analysis of computational complexity:

a) *Time complexity*: Assuming the model has a total of M parameters and the input x has dimensions $(3, 224, 224)$, denoted by $P = 3 \times 224 \times 224$. The estimated theoretical time complexity of our proposed method is as follows:

- Stage 1. Train Model: Update model parameters: $O(MP)$ [42]
- Stage 2. Update perturbation
 - Step 1. Perform a forward pass to obtain the Loss: $O(MP)$
 - Step 2. Calculate the Jacobian matrix of the Loss with respect to $x + \delta$: $O(P)$
 - Step 3. Use the HVP (Hessian-vector Product) to estimate Hv : $O(P)$ (Or directly calculate the Hessian: $O(P^2)$)
 - Step 4. Compute $\text{tr}(H^T H)$ or $\|Hv\|_F$: $O(P)$
 - Step 5. Backpropagate and update ϵ : $O(P)$

In summary, generating perturbations using the original method has an overall time complexity of $O(MP) + O(P^2) + O(P)$, while using HVP reduces the time complexity to $O(MP) + O(P)$.

b) *Space complexity*: Since the space complexity of our proposed algorithm is independent of the model, we assume that the space complexity of Stage 1 is fixed at O_1 . We will primarily analyze the space complexity of the Hessian part.

After obtaining the Jacobian matrix of the loss function with respect to $X + \delta$, whose space complexity is $O(P)$, the original method computes the gradient of each element of the Jacobian matrix with respect to $X + \delta$, resulting in a computational complexity of $O(P^2)$. However, HVP first uses a vector v as a weight matrix to compute a weighted sum of the Jacobian matrix, then uses PyTorch's computation graph to perform backpropagation on $X + \delta$ to approximate Hv , this process maintains a space complexity of $O(P)$.

In summary, we reduce the space complexity of the Hessian part from $O(P^2)$ to $O(P)$. Specifically, for ImageNet images, generating perturbations requires 13,842 MiB of GPU memory.

IV. EXPERIMENTS

In this section, we verify the effectiveness, transferability, and stealthiness of the poisoning perturbations generated by DPA, and verify the performance of HVP. In addition, we also challenge our method with some defense strategies such as data augmentation methods or limited poisoning percentages. Finally, we propose a new training paradigm for DPA to enhance the robustness of the model and compare it with traditional adversarial training.

A. Experiment setting

a) *Datasets & Models*: We generate perturbation on the CIFAR10 [43], SVHN [44], and TinyImageNet [4] datasets respectively. Subsequently, we use the VGG16 [45], ResNet18 [46], and ResNet50 [46] models to train on the CIFAR10 and SVHN datasets. For the TinyImageNet, we use the ResNet18, ResNet50, and DenseNet121 [47] models for training. It should be noted that the TinyImageNet is a subset of the ImageNet dataset.

b) *Evaluation metric*: The major claim of our work is that models trained over a dataset poisoned by our DPA would exhibit a lower robustness against adversarial perturbation or even natural noises. Thus we quantize the robustness of a victim model by adopting the measure defined by [48]. That is,

$$\hat{\rho}(f) = \frac{1}{|\mathcal{D}|} \sum_{x \in \mathcal{D}} \frac{\|\hat{r}(x)\|_p}{\|x\|_p} \quad (6)$$

where $\hat{r}(x)$ is the minimal perturbation for a successful attack, and \mathcal{D} denotes the validation set. p is 2 (e.g., DeepFool [48]) or ∞ (e.g., FGSM and PGD). A smaller $\hat{\rho}(f)$ indicates a model is more vulnerable.

On the other hand, we emphasize that our DPA could significantly decrease the degradation of the model performance on clean examples, exhibiting the stealthiness of our DPA. To this end, we apply traditional poisoning methods such as EM [49], REM [50], LSP [51], and AR [52], as well as our proposed method to contaminate datasets [15]. We assess the classification accuracy of the poisoned models, the closer the accuracy is to that of the clean models, the more effective the stealth of the poisoning attack method.

B. Effectiveness of deferred poisoning attack

We claim that the model trained over the dataset poisoned by our DPA could function normally on the validation dataset but is significantly vulnerable to adversarial noise or even natural noise. We support our main claim with the experiment results as follows.

As shown in Table I where $\hat{\rho}_F$, $\hat{\rho}_P$ and $\hat{\rho}_D$ represent the robustness of victim models attacked by FGSM, PGD, and DeepFool respectively, we can observe that the ACC of both the clean models and the poisoned models are almost the same. For example, the 4th and 5th rows, corresponding to the 1st to 4th columns, illustrate the performance of the model trained with ResNet18 on TinyImageNet. After being subjected to DPA, the poisoned model maintains the same accuracy as the clean model on the validation set, both at 0.72. However, the robustness of the poisoned model against FGSM, PGD, and DeepFool adversarial attacks has significantly decreased from 0.74, 0.50, and 0.28 to 0.48, 0.42, and 0.09, respectively. Similarly, by examining the data for other models and datasets in the table, we arrive at the same conclusion.

a) *Transferability*: It is important to note that, in these examples from Table I, perturbations are generated based on the VGG16 model that was pretrained on the full ImageNet dataset. However, the toxic effects of these perturbations are

TABLE I: The comparison of the accuracy and robustness(%) of the clean model and poisoned model against different kinds of evasion attacks.

	ACC	$\hat{\rho}_F \downarrow$	$\hat{\rho}_P \downarrow$	$\hat{\rho}_D \downarrow$	ACC	$\hat{\rho}_F \downarrow$	$\hat{\rho}_P \downarrow$	$\hat{\rho}_D \downarrow$	ACC	$\hat{\rho}_F \downarrow$	$\hat{\rho}_P \downarrow$	$\hat{\rho}_D \downarrow$
Dataset-Model	TinyImageNet-DesNet121				CIFAR10-VGG16				SVHN-VGG16			
Clean	0.74	0.75	0.48	0.24	0.89	1.86	0.94	1.19	0.95	3.83	1.98	5.39
Poisoned	0.73	0.58	0.42	0.08	0.75	0.58	0.50	0.32	0.88	1.54	0.93	1.10
Dataset-Model	TinyImageNet-ResNet18				CIFAR10-ResNet18				SVHN-ResNet18			
Clean	0.72	0.74	0.50	0.28	0.81	1.62	1.01	1.24	0.94	3.33	1.73	2.57
Poisoned	0.72	0.48	0.42	0.09	0.76	0.79	0.57	0.39	0.89	1.78	1.03	1.24
Dataset-Model	TinyImageNet-ResNet50				CIFAR10-ResNet50				SVHN-ResNet50			
Clean	0.73	0.82	0.49	0.23	0.78	2.84	1.48	1.21	0.92	3.24	1.59	2.48
Poisoned	0.72	0.50	0.43	0.07	0.73	1.38	0.62	0.45	0.88	1.63	0.97	1.16

not only effective on the VGG16 model (white-box scenario) but also transfer to other models such as ResNet18, ResNet50, and DenseNet121 (black-box scenarios). This indicates that DPA possesses excellent transferability, thereby making it highly suitable for black-box attack scenarios. The poisoned model being simultaneously affected by adversarial samples and natural noise indicates that DPA fundamentally reduces the model's robustness to arbitrary perturbations. This corroborates our claim that by increasing the curvature of the loss function around local optima, the model becomes more vulnerable.

b) *Generalized scenario*: Adversarial examples do not frequently manifest in real-world scenarios. According to our claim, DPA fundamentally reduces the model's robustness to arbitrary perturbations, that's means poisoned model not only simultaneously affected by adversarial samples but also natural noise. To substantiate this, we introduce random noise sampled from different distributions to the test images to simulate more general conditions as shown in Fig. 5.



Fig. 5: Image after adding different random noise

We experimented with natural noise from various distributions:

- **Gaussian Noise**: Gaussian Noise follows a normal distribution and is the most common type of noise found in the real world;
- **Poisson Noise**: Poisson Noise is a type of discrete noise that can simulate the imaging process under low-light conditions;
- **Speckle Noise**: Speckle Noise is typically related to the local brightness of an image and can simulate bright or dark spots that may appear in an image;
- **Rayleigh Noise**: Rayleigh Noise can simulate image degradation caused by atmospheric scattering or other similar effects, typically manifesting as fluctuations in image brightness, particularly in the edge regions of the image;

TABLE II: The impact of natural noise on the poisoned and clean models.

Noise		Clean	Gaussian	Poisson	Speckle	Rayleigh
VGG16	Clean	0.89	0.80	0.71	0.72	0.82
	Poisoned	0.75	0.45	0.47	0.48	0.44
ResNet18	Clean	0.81	0.60	0.63	0.62	0.66
	Poisoned	0.76	0.41	0.49	0.41	0.43
ResNet50	Clean	0.78	0.63	0.61	0.65	0.68
	Poisoned	0.73	0.37	0.50	0.38	0.42

Table II compares the classification accuracy of clean and poisoned models on CIFAR10 with different sampled random noise injections. It is evident that the poisoned models are significantly more sensitive to random noise, indicating that our method can render the models vulnerable. For example, in the second column, when perturbing VGG16 with Gaussian noise, the clean model achieves a high classification accuracy of 0.80, remaining virtually unaffected by the noise. However, when the same Gaussian noise is used to disturb the poisoned model, the classification accuracy drops to only 0.45. This indicates that DPA renders the model considerably vulnerable even to natural noise, and poses a significant potential threat to the field of artificial intelligence security.

C. Stealthiness of poisoned samples

Similar to traditional poisoning attacks, we aim for the poisoned samples generated by DPA to be imperceptible to the human eye. In this section, we verify the low attack cost characteristic of DPA and thereby achieve the stealthiness of the poisoned samples.

DPA has a significant advantage over traditional data poisoning methods, it requires only a minimal perturbation cost, such as $\epsilon = 3/255$, to achieve excellent results. In contrast, data poisoning methods with l_∞ norm constraints, such as EM and REM, do not demonstrate effectiveness at this level of perturbation.

By contrasting the classification accuracy of adversarial samples between the poisoned and clean models, we present the effectiveness of DPA in a more intuitive form. Table III presents the classification accuracy of the model against different adversarial samples after being subjected to poisoning attacks with varying perturbation radii, it shows that the EM and REM methods do not fully take effect when ϵ are as low as $3/255$ or even $5/255$ across different models, at least $\epsilon = 8/255$ to exhibit aggressiveness. In contrast, our method

TABLE III: The performance of various poisoning attacks at different attack scales.

Dataset		CIFAR10($\epsilon = \frac{3}{255} / \frac{5}{255} / \frac{8}{255}$)				SVHN($\epsilon = \frac{3}{255} / \frac{5}{255} / \frac{8}{255}$)			
Model	Method	Clean data	FGSM↓	PGD↓	CW↓	Clean data	FGSM↓	PGD↓	CW↓
VGG16	Clean	0.89	0.65	0.71	0.66	0.95	0.84	0.88	0.84
	EM	0.87/0.83/0.27	0.62/0.49/-	0.68/0.54/-	0.64/0.44/-	0.93/0.93/0.29	0.80/0.79/-	0.84/0.83/-	0.79/0.78/-
	REM	0.87/0.54/0.39	0.61/-/-	0.67/-/-	0.62/-/-	0.93/0.93/0.93	0.79/0.80/0.79	0.83/0.84/0.83	0.78/0.79/0.79
	Ours	0.75/0.69/0.67	0.14/0.17/0.20	0.21/0.23/0.28	0.14/0.18/0.21	0.88/0.83/0.76	0.45/0.41/0.41	0.53/0.50/0.48	0.43/0.40/0.38
ResNet18	Clean	0.81	0.60	0.65	0.60	0.94	0.79	0.83	0.79
	EM	0.77/0.66/0.37	0.55/0.27/-	0.60/0.31/-	0.56/0.22/-	0.91/0.44/0.27	0.73/-/-	0.78/-/-	0.72/-/-
	REM	0.78/0.40/0.38	0.56/-/-	0.61/-/-	0.57/-/-	0.91/0.17/0.42	0.73/-/-	0.78/-/-	0.73/-/-
	Ours	0.76/0.72/0.70	0.24/0.19/0.18	0.32/0.27/0.25	0.23/0.19/0.17	0.89/0.83/0.73	0.54/0.45/0.44	0.61/0.53/0.50	0.51/0.42/0.41
ResNet50	Clean	0.78	0.58	0.63	0.59	0.92	0.76	0.81	0.75
	EM	0.76/0.74/0.32	0.55/0.52/-	0.60/0.57/-	0.56/0.53/-	0.90/0.40/0.24	0.70/-/-	0.76/-/-	0.70/-/-
	REM	0.75/0.71/0.47	0.54/0.44/-	0.60/0.49/-	0.56/0.44/-	0.89/0.46/0.32	0.72/-/-	0.76/-/-	0.72/-/-
	Ours	0.73/0.71/0.66	0.29/0.17/0.16	0.37/0.24/0.23	0.29/0.16/0.16	0.88/0.80/0.74	0.47/0.42/0.37	0.55/0.50/0.44	0.44/0.39/0.34

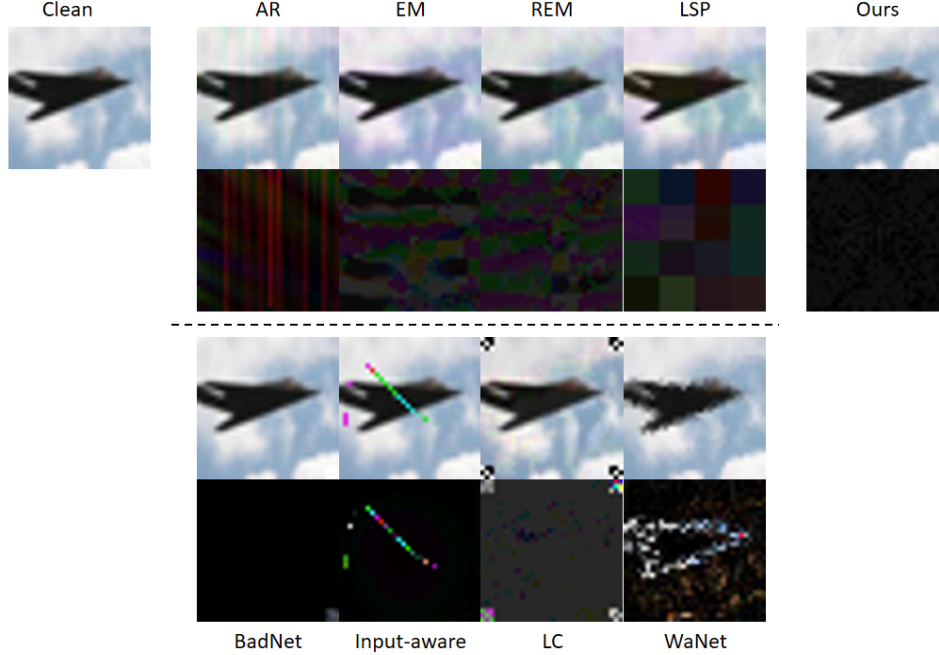


Fig. 6: Comparison of examples generated by different Poisoning attacks above the dotted line(i.e. AR, EM, REM and LSP) and Backdoor attack below the dotted line(i.e. BadNet, Input-aware, LC and WaNet). For each attack, we show the poisoned sample (top) and the magnified ($\times 5$) residual (bottom).

shows excellent offensiveness even at the scale of $\epsilon = 3/255$. For instance, in rows 2 to 4 of Table III for the VGG16 model trained on CIFAR10, when $\epsilon = 3/255$, the models trained with EM and REM maintain high classification accuracy and accuracy post-adversarial attack. However, the model poisoned by DPA exhibits extremely low accuracy post-adversarial attack, indicating that the models are very vulnerable and can be significantly impacted by adversarial examples due to the approach mentioned. This also suggests that the attack cost of DPA is much lower than that of traditional poisoning attacks, while also ensuring the stealthiness of our method.

Aiming to assess stealthiness without compromising the efficacy of poisoning attacks, we set the l_∞ norm attacks' parameter ϵ to $8/255$ for traditional poisoning attacks, such as EM and REM. For l_2 norm attacks, such as AR and LSP, we set ϵ to 1. However, for DPA, an ϵ setting of $3/255$ is sufficient to ensure aggressiveness.

As depicted in Fig. 6, the perturbation we propose is difficult to discern with the naked eye. Compared to other poisoning

and backdoor attacks, even when the residual images between the poisoned and clean images are magnified five times, the noise is hardly noticeable. This illustrates the profound visual stealthiness inherent in our method, which is alarming in terms of its potential for misuse.

D. Comparison with backdoor attacks

Similar to DPA, models attacked by backdoor attacks behave normally during the training phase. Backdoor attacks are executed by introducing specific backdoors into the training samples, which prompts the model to learn the relationship between the backdoor and a designated label. This leads to the model exhibiting abnormal behavior during the testing phase when it encounters the trigger. However, DPA does not implant specific Trojans, more generally, its goal is to make poisoned models particularly vulnerable, primarily by making them more susceptible to adversarial attacks even random noise.

Table IV demonstrates that even when the attack success rate (ASR) is very high, backdoor attacks do not render the

TABLE IV: The accuracy and robustness(%) of VGG16 after training CIFAR10 with backdoors implanted.

Methods	Robustness	ACC	ASR	$\hat{\rho}_F \downarrow$	$\hat{\rho}_P \downarrow$	$\hat{\rho}_D \downarrow$
Clean		0.89	-	1.86	0.94	1.19
BadNet		0.83	0.95	1.51	0.78	0.80
Input-aware		0.84	0.87	1.57	0.84	0.92
LC		0.85	0.90	1.41	0.76	0.74
WaNet		0.84	0.58	2.29	0.78	0.64
SAPA		0.87	0.77	1.34	0.85	1.01
Ours		0.75	-	0.58	0.50	0.32

model more vulnerable. This indicates that the aggressiveness of deferred poisoning attack is insidious and unique, it can make the model more vulnerable while ensuring normal model performance, bringing unforeseen potential harm to machine learning.

E. Robustness analysis

We conduct various data augmentation techniques [53], [54] on data-infused with deferred poison. By observing the performance of models trained on these augmented datasets, we assess the robustness of DPA. Specifically, in addition to augmenting the images, we compare the effects of models both before and after they utilize weights pre-trained on ImageNet.

Table V displays the performance of deferred poisoning attacks when facing various data augmentation techniques with ϵ set to 3/255. It is evident that our method can still render models vulnerable under most data augmentation methods as well as with pre-trained models, indicating that our approach possesses strong robustness.

F. Different poisoning percentages

In real-world scenarios, it is highly probable that attackers do not have complete access to all data. More challengingly, we simulate the hazards of deferred poisoning attacks under various realistic conditions using different percentages of poisoned data.

Table VI displays the performance of the VGG16 model under various percentages of deferred poisoning attacks on the CIFAR10 dataset. As the poisoning ratio increases, the model becomes increasingly vulnerable. When the poisoning ratio reaches 40%, the deferred poisoning attack has already demonstrated its offensiveness. Even at a ratio of 60%, the model suffers significant harm, which further illustrates the severe threat that deferred poisoning attacks pose to machine learning, poisoning only a portion of the training data can pose a serious risk to the model.

G. Hessian-vector product performance

In Section III-D, we introduce the Hessian-vector product (HVP) to calculate the relaxed solution of the Hessian singularization term more quickly. With the new strategy, it now takes about 240 minutes to poison the entire CIFAR10, and about 30 hours to Tiny-ImageNet for large-scale scenarios, which is comparable to the competitive methods in our paper as shown in Table VII.

For example, as shown in the 1st-3rd row of the 1st column of Table VII, when training CIFAR10 with VGG16 after being

attacked by the original DPA, the model's robustness under FGSM attack drops from 1.86% to 0.54%. In contrast, when training with the dataset under HVP rapid attack, the robustness is 0.58%, which is close to the original attack method. This indicates that HVP can accelerate the poisoning process without compromising the effectiveness of the DPA attack.

H. Adversarial training

Adversarial training has emerged as a pivotal technique for enhancing the robustness of models, particularly when it comes to safeguarding against adversarial attacks. For example, Madry et al. [18] train the model to minimize loss function under adversarial perturbations by using Projected Gradient Descent (PGD) as an adversary, thereby enhancing the model's robustness against a broad range of adversarial attacks. Foret et al. [36] enhance model's generalization by concurrently reducing both its loss value and the sharpness of the loss landscape.

Table VIII demonstrates the effectiveness of DPA attacks against various adversarial training methods, where AT denotes adversarial training using PGD [18]. As shown in the 4th row of the 6th column, traditional adversarial training methods are not entirely effective in defending against our attacks. For instance, when training CIFAR10 with VGG16 and under the FGSM attack, the robustness of the clean model is 1.86%, whereas the robustness of the model poisoned after adversarial training is only 0.71%.

The results also show that SAM is ineffective against our attack method. For example, the model robustness of VGG16-CIFAR10, with and without SAM adversarial training, is nearly the same, 0.57% (the 4th row of the 3rd column) and 0.58% (the 5th row of the 3rd column), respectively. SAM is ineffective possibly because it focuses on decreasing the curvature of the loss function with respect to model parameters. In contrast, our method aims to increase the curvature of the loss function concerning the input examples. They are two different dimensionalities of the loss function. Therefore, SAM cannot effectively counter our attack method.

Consequently, we propose a new training paradigm that directly decreasing the curvature of the loss function with respect to the input (namely, **Ours** in Table VIII). For example, in the 2nd row and the 5th row of the table, the robustness increases from 0.58% to 1.72%. This finding warns researchers that simply adopting commonly used adversarial training strategies is not enough to ensure a trustworthy model. Considering the curvature information maliciously used by our DPA is also crucial. In summary, our work focuses on revealing a new attack. Like most pioneering works (e.g., FGSM, PGD) in adversarial machine learning, we present a novel attack method, and a defense method naturally follows to design a more robust model.

V. CONCLUSION

In this paper, we introduce the Deferred Poisoning Attack (DPA), a stealthy threat in artificial intelligence that performs normally during training and validation. DPA targets the Hessian matrix, inducing a rapid convergence to a steep

TABLE V: The accuracy and robustness(%) of poisoned models over CIFAR10 after data augmentation.

Method	Robustness				VGG16				ResNet18				ResNet50			
	ACC	$\hat{\rho}_F \downarrow$	$\hat{\rho}_P \downarrow$	$\hat{\rho}_D \downarrow$	ACC	$\hat{\rho}_F \downarrow$	$\hat{\rho}_P \downarrow$	$\hat{\rho}_D \downarrow$	ACC	$\hat{\rho}_F \downarrow$	$\hat{\rho}_P \downarrow$	$\hat{\rho}_D \downarrow$	ACC	$\hat{\rho}_F \downarrow$	$\hat{\rho}_P \downarrow$	$\hat{\rho}_D \downarrow$
Clean	0.89	1.86	0.94	1.19	0.81	1.62	1.01	1.24	0.78	2.84	1.48	1.21	0.78	2.84	1.48	1.21
Standard	0.75	0.58	0.50	0.32	0.76	0.79	0.57	0.39	0.73	1.38	0.62	0.45	0.73	1.38	0.62	0.45
Pretrained	0.78	0.85	0.53	0.35	0.75	1.12	0.59	0.42	0.72	0.66	0.55	0.34	0.72	0.66	0.55	0.34
Cutout	0.77	0.61	0.50	0.34	0.77	0.92	0.60	0.44	0.75	1.45	0.59	0.41	0.75	1.45	0.59	0.41
Gaussian	0.75	0.55	0.49	0.32	0.78	0.87	0.58	0.42	0.74	1.39	0.63	0.41	0.74	1.39	0.63	0.41
Gray	0.72	0.60	0.49	0.32	0.73	0.62	0.53	0.35	0.69	0.82	0.58	0.35	0.69	0.82	0.58	0.35
JPEG	0.78	0.85	0.58	0.45	0.79	1.16	0.64	0.60	0.78	0.98	0.60	0.49	0.78	0.98	0.60	0.49

TABLE VI: The accuracy and robustness(%) of VGG16 under different poisoning percentages in CIFAR10.

Robustness	Percentage					
	0%	20%	40%	60%	80%	100%
ACC	0.89	0.88	0.87	0.86	0.83	0.75
$\hat{\rho}_F \downarrow$	1.86	2.53	1.35	1.06	1.08	0.58
$\hat{\rho}_P \downarrow$	0.94	0.97	0.71	0.65	0.63	0.50
$\hat{\rho}_D \downarrow$	1.19	1.03	0.73	0.65	0.56	0.32

TABLE VII: The comparison of the robustness(%) compared with the origin method and HVP.

		CIFAR10				SVHN			
		ACC	$\hat{\rho}_F \downarrow$	$\hat{\rho}_P \downarrow$	$\hat{\rho}_D \downarrow$	ACC	$\hat{\rho}_F \downarrow$	$\hat{\rho}_P \downarrow$	$\hat{\rho}_D \downarrow$
VGG16	Clean	0.90	1.86	0.94	1.19	0.95	3.98	1.98	5.39
	Origin	0.72	0.54	0.45	0.30	0.83	1.42	0.86	1.04
	HVP	0.75	0.58	0.50	0.32	0.89	1.54	0.93	1.10
ResNet18	Clean	0.81	1.62	1.01	1.24	0.94	3.33	1.73	2.57
	Origin	0.74	0.72	0.49	0.31	0.84	1.65	0.96	1.12
	HVP	0.76	0.79	0.57	0.39	0.89	1.78	1.03	1.24
ResNet50	Clean	0.79	2.84	1.48	1.21	0.92	3.24	1.59	2.48
	Origin	0.70	1.28	0.51	0.38	0.84	1.54	0.93	1.12
	HVP	0.73	1.38	0.62	0.45	0.88	1.63	0.97	1.16

local optimum on poisoned data, thereby diminishing the model's robustness. We demonstrate DPA's effectiveness and stealth through comparative adversarial analyses with traditional attacks. Notably, DPA demands lower costs and exhibits transferability. We also establish its resilience against common augmentations and pretrained defenses, highlighting its universal risk underscores a novel challenge for AI security.

REFERENCES

- [1] K. He, X. Zhang, S. Ren, and J. Sun, "Deep residual learning for image recognition," in *Proceedings of the IEEE conference on computer vision and pattern recognition*, 2016, pp. 770–778.
- [2] A. Vaswani, N. Shazeer, N. Parmar, J. Uszkoreit, L. Jones, A. N. Gomez, E. Kaiser, and I. Polosukhin, "Attention is all you need," *Advances in neural information processing systems*, vol. 30, 2017.
- [3] R. Rombach, A. Blattmann, D. Lorenz, P. Esser, and B. Ommer, "High-resolution image synthesis with latent diffusion models," in *Proceedings of the IEEE/CVF conference on computer vision and pattern recognition*, 2022, pp. 10684–10695.
- [4] O. Russakovsky, J. Deng, H. Su, J. Krause, S. Satheesh, S. Ma, Z. Huang, A. Karpathy, A. Khosla, M. Bernstein *et al.*, "Imagenet large scale visual recognition challenge," *International journal of computer vision*, vol. 115, pp. 211–252, 2015.
- [5] T.-Y. Lin, M. Maire, S. Belongie, J. Hays, P. Perona, D. Ramanan, P. Dollár, and C. L. Zitnick, "Microsoft coco: Common objects in context," in *Computer Vision—ECCV 2014: 13th European Conference, Zurich, Switzerland, September 6–12, 2014, Proceedings, Part V 13*. Springer, 2014, pp. 740–755.
- [6] Y. Taigman, M. Yang, M. Ranzato, and L. Wolf, "Deepface: Closing the gap to human-level performance in face verification," in *Proceedings of the IEEE conference on computer vision and pattern recognition*, 2014, pp. 1701–1708.
- [7] L. Tao, L. Feng, J. Yi, S.-J. Huang, and S. Chen, "Better safe than sorry: Preventing delusive adversaries with adversarial training," *Advances in Neural Information Processing Systems*, vol. 34, pp. 16 209–16 225, 2021.
- [8] L. Fowl, M. Goldblum, P.-y. Chiang, J. Geiping, W. Czaja, and T. Goldstein, "Adversarial examples make strong poisons," *Advances in Neural Information Processing Systems*, vol. 34, pp. 30 339–30 351, 2021.
- [9] L. Tao, L. Feng, H. Wei, J. Yi, S.-J. Huang, and S. Chen, "Can adversarial training be manipulated by non-robust features?" *Advances in Neural Information Processing Systems*, vol. 35, pp. 26 504–26 518, 2022.
- [10] A. Shafahi, W. R. Huang, M. Najibi, O. Suci, C. Studer, T. Dumitras, and T. Goldstein, "Poison frogs! targeted clean-label poisoning attacks on neural networks," in *Advances in Neural Information Processing Systems*, S. Bengio, H. Wallach, H. Larochelle, K. Grauman, N. Cesa-Bianchi, and R. Garnett, Eds., vol. 31. Curran Associates, Inc., 2018. [Online]. Available: https://proceedings.neurips.cc/paper_files/paper/2018/file/22722a343513ed45f14905eb07621686-Paper.pdf
- [11] H. Huang, X. Ma, S. M. Erfani, J. Bailey, and Y. Wang, "Unlearnable examples: Making personal data unexploitable," *arXiv preprint arXiv:2101.04898*, 2021.
- [12] S. Fu, F. He, Y. Liu, L. Shen, and D. Tao, "Robust unlearnable examples: Protecting data against adversarial learning," *arXiv preprint arXiv:2203.14533*, 2022.
- [13] M. Fang, X. Cao, J. Jia, and N. Z. Gong, "Local model poisoning attacks to byzantine-robust federated learning," in *USENIX Security Symposium*, 2019. [Online]. Available: <https://api.semanticscholar.org/CorpusID:208310035>
- [14] T. Bai, J. Luo, J. Zhao, B. Wen, and Q. Wang, "Recent advances in adversarial training for adversarial robustness," *arXiv preprint arXiv:2102.01356*, 2021.
- [15] T. Qin, X. Gao, J. Zhao, K. Ye, and C.-Z. Xu, "Apbench: A unified benchmark for availability poisoning attacks and defenses," *arXiv preprint arXiv:2308.03258*, 2023.
- [16] F. Liao, M. Liang, Y. Dong, T. Pang, X. Hu, and J. Zhu, "Defense against adversarial attacks using high-level representation guided denoiser," in *Proceedings of the IEEE conference on computer vision and pattern recognition*, 2018, pp. 1778–1787.
- [17] I. J. Goodfellow, J. Shlens, and C. Szegedy, "Explaining and harnessing adversarial examples," *arXiv preprint arXiv:1412.6572*, 2014.
- [18] A. Madry, A. Makelov, L. Schmidt, D. Tsipras, and A. Vladu, "Towards deep learning models resistant to adversarial attacks," *arXiv preprint arXiv:1706.06083*, 2017.
- [19] S. P. Boyd and L. Vandenberghe, *Convex optimization*. Cambridge university press, 2004.
- [20] B. Biggio, B. Nelson, and P. Laskov, "Poisoning attacks against support vector machines," *arXiv preprint arXiv:1206.6389*, 2012.
- [21] B. Biggio and F. Roli, "Wild patterns: Ten years after the rise of adversarial machine learning," *Proceedings of the 2018 ACM SIGSAC Conference on Computer and Communications Security*, 2017. [Online]. Available: <https://api.semanticscholar.org/CorpusID:53107276>
- [22] M. Jagielski, A. Oprea, B. Biggio, C. Liu, C. Nita-Rotaru, and B. Li, "Manipulating machine learning: Poisoning attacks and countermeasures for regression learning," *2018 IEEE Symposium on Security and Privacy (SP)*, pp. 19–35, 2018. [Online]. Available: <https://api.semanticscholar.org/CorpusID:4551073>
- [23] Y. Liu, S. Ma, Y. Aafer, W.-C. Lee, J. Zhai, W. Wang, and X. Zhang, "Trojaning attack on neural networks," in *Network and Distributed System Security Symposium*, 2018. [Online]. Available: <https://api.semanticscholar.org/CorpusID:31806516>
- [24] S. Fu, F. He, Y. Liu, L. Shen, and D. Tao, "Robust unlearnable examples: Protecting data against adversarial learning," *arXiv preprint arXiv:2203.14533*, 2022.
- [25] P. He, H. Xu, J. Ren, Y. Cui, S. Zeng, H. Liu, C. C. Aggarwal, and J. Tang, "Sharpness-aware data poisoning attack," in *The Twelfth*

TABLE VIII: The comparison of the accuracy and robustness(%) of different kinds of adversarial training method against DPA.

	ACC	$\hat{\rho}_F \uparrow$	$\hat{\rho}_P \uparrow$	$\hat{\rho}_D \uparrow$	ACC	$\hat{\rho}_F \uparrow$	$\hat{\rho}_P \uparrow$	$\hat{\rho}_D \uparrow$	ACC	$\hat{\rho}_F \uparrow$	$\hat{\rho}_P \uparrow$	$\hat{\rho}_D \uparrow$
	VGG16-CIFAR10				ResNet18-CIFAR10				ResNet50-CIFAR10			
Clean	0.89	1.86	0.94	1.19	0.81	1.62	1.01	1.24	0.78	2.84	1.48	1.21
No defense	0.75	0.58	0.50	0.32	0.76	0.79	0.57	0.39	0.74	1.38	0.62	0.45
SAM	0.76	0.57	0.50	0.30	0.79	0.84	0.57	0.41	0.78	0.98	0.57	0.39
AT	0.78	0.71	0.77	0.94	0.79	1.07	0.78	0.79	0.78	1.51	0.86	0.87
Ours	0.80	1.72	1.25	1.52	0.71	1.93	1.31	1.54	0.68	2.51	1.54	1.83

International Conference on Learning Representations, 2024. [Online]. Available: <https://openreview.net/forum?id=bxITGFPVWh>

- [26] E. Bagdasaryan, A. Veit, Y. Hua, D. Estrin, and V. Shmatikov, “How to backdoor federated learning,” *ArXiv*, vol. abs/1807.00459, 2018. [Online]. Available: <https://api.semanticscholar.org/CorpusID:49557410>
- [27] Y. Liu, W.-C. Lee, G. Tao, S. Ma, Y. Aafer, and X. Zhang, “Abs: Scanning neural networks for back-doors by artificial brain stimulation,” *Proceedings of the 2019 ACM SIGSAC Conference on Computer and Communications Security*, 2019. [Online]. Available: <https://api.semanticscholar.org/CorpusID:204746801>
- [28] H. Chen, C. Fu, J. Zhao, and F. Koushanfar, “Deepinspect: A black-box trojan detection and mitigation framework for deep neural networks,” in *International Joint Conference on Artificial Intelligence*, 2019. [Online]. Available: <https://api.semanticscholar.org/CorpusID:199466093>
- [29] Y. Liu, X. Ma, J. Bailey, and F. Lu, “Reflection backdoor: A natural backdoor attack on deep neural networks,” *ArXiv*, vol. abs/2007.02343, 2020. [Online]. Available: <https://api.semanticscholar.org/CorpusID:220363879>
- [30] S. Kolouri, A. Saha, H. Pirsiavash, and H. Hoffmann, “Universal litmus patterns: Revealing backdoor attacks in cnns,” *2020 IEEE/CVF Conference on Computer Vision and Pattern Recognition (CVPR)*, pp. 298–307, 2019. [Online]. Available: <https://api.semanticscholar.org/CorpusID:195658208>
- [31] T. Gu, B. Dolan-Gavitt, and S. Garg, “Badnets: Identifying vulnerabilities in the machine learning model supply chain,” *arXiv preprint arXiv:1708.06733*, 2017.
- [32] A. Turner, D. Tsipras, and A. Madry, “Label-consistent backdoor attacks,” *arXiv preprint arXiv:1912.02771*, 2019.
- [33] T. A. Nguyen and A. Tran, “Input-aware dynamic backdoor attack,” *Advances in Neural Information Processing Systems*, vol. 33, pp. 3454–3464, 2020.
- [34] T. A. Nguyen and A. T. Tran, “Wanet - imperceptible warping-based backdoor attack,” in *International Conference on Learning Representations*, 2021. [Online]. Available: <https://openreview.net/forum?id=eEn8KTJ0X>
- [35] Y. Zhao, H. Zhang, and X. Hu, “Penalizing gradient norm for efficiently improving generalization in deep learning,” in *International Conference on Machine Learning*. PMLR, 2022, pp. 26982–26992.
- [36] P. Foret, A. Kleiner, H. Mobahi, and B. Neyshabur, “Sharpness-aware minimization for efficiently improving generalization,” in *International Conference on Learning Representations*, 2021. [Online]. Available: <https://openreview.net/forum?id=6TmImposlRM>
- [37] S. Wu, S. Chen, C. Xie, and X. Huang, “One-pixel shortcut: on the learning preference of deep neural networks,” *arXiv preprint arXiv:2205.12141*, 2022.
- [38] H. He, K. Zha, and D. Katabi, “Indiscriminate poisoning attacks on unsupervised contrastive learning,” *arXiv preprint arXiv:2202.11202*, 2022.
- [39] Z. Tian, L. Cui, J. Liang, and S. Yu, “A comprehensive survey on poisoning attacks and countermeasures in machine learning,” *ACM Computing Surveys*, vol. 55, no. 8, pp. 1–35, 2022.
- [40] L. Muñoz-González, B. Biggio, A. Demontis, A. Paudice, V. Wongrasamee, E. C. Lupu, and F. Roli, “Towards poisoning of deep learning algorithms with back-gradient optimization,” in *Proceedings of the 10th ACM workshop on artificial intelligence and security*, 2017, pp. 27–38.
- [41] P. Lancaster and M. Tismenetsky, *The theory of matrices: with applications*. Elsevier, 1985.
- [42] B. Shah and H. Bhavsar, “Time complexity in deep learning models,” *Procedia Computer Science*, vol. 215, pp. 202–210, 2022.
- [43] A. Krizhevsky, G. Hinton *et al.*, “Learning multiple layers of features from tiny images,” 2009.
- [44] Y. Netzer, T. Wang, A. Coates, A. Bissacco, B. Wu, A. Y. Ng *et al.*, “Reading digits in natural images with unsupervised feature learning,” in *NIPS workshop on deep learning and unsupervised feature learning*, vol. 2011, no. 5. Granada, Spain, 2011, p. 7.
- [45] K. Simonyan and A. Zisserman, “Very deep convolutional networks for large-scale image recognition,” *arXiv preprint arXiv:1409.1556*, 2014.
- [46] K. He, X. Zhang, S. Ren, and J. Sun, “Deep residual learning for image recognition,” in *Proceedings of the IEEE conference on computer vision and pattern recognition*, 2016, pp. 770–778.
- [47] G. Huang, Z. Liu, L. Van Der Maaten, and K. Q. Weinberger, “Densely connected convolutional networks,” in *Proceedings of the IEEE conference on computer vision and pattern recognition*, 2017, pp. 4700–4708.
- [48] S.-M. Moosavi-Dezfooli, A. Fawzi, and P. Frossard, “Deepfool: a simple and accurate method to fool deep neural networks,” in *Proceedings of the IEEE conference on computer vision and pattern recognition*, 2016, pp. 2574–2582.
- [49] H. Huang, X. Ma, S. M. Erfani, J. Bailey, and Y. Wang, “Unlearnable examples: Making personal data unexploitable,” *arXiv preprint arXiv:2101.04898*, 2021.
- [50] S. Fu, F. He, Y. Liu, L. Shen, and D. Tao, “Robust unlearnable examples: Protecting data against adversarial learning,” *arXiv preprint arXiv:2203.14533*, 2022.
- [51] D. Yu, H. Zhang, W. Chen, J. Yin, and T.-Y. Liu, “Availability attacks create shortcuts,” in *Proceedings of the 28th ACM SIGKDD Conference on Knowledge Discovery and Data Mining*, 2022, pp. 2367–2376.
- [52] P. Sandoval-Segura, V. Singla, J. Geiping, M. Goldblum, T. Goldstein, and D. Jacobs, “Autoregressive perturbations for data poisoning,” *Advances in Neural Information Processing Systems*, vol. 35, pp. 27374–27386, 2022.
- [53] T. DeVries and G. W. Taylor, “Improved regularization of convolutional neural networks with cutout,” *arXiv preprint arXiv:1708.04552*, 2017.
- [54] Z. Liu, Z. Zhao, and M. Larson, “Image shortcut squeezing: Countering perturbative availability poisons with compression,” in *International conference on machine learning*. PMLR, 2023, pp. 22473–22487.